Eur. Phys. J. B **34**, 473–478 (2003)
DOI: 10.1140/epjb/e2003-00246-8

THE EUROPEAN
PHYSICAL JOURNAL B

Theory and simulation of positionally frozen Heisenberg spin systems

E. Lomba[a], C. Martín, and N.G. Almarza

Instituto de Química Física Rocasolano (CSIC), Serrano 119, 28006 Madrid, Spain

Received 27 March 2003 / Received in final form 25 July 2003
Published online 9 September 2003 –

Abstract. The structure, thermodynamics and the ferromagnetic phase transition of a positionally frozen disordered Heisenberg spin system are studied by means of extensive Monte Carlo calculations in combination with finite size scaling techniques, as well as resorting to the Replica Ornstein-Zernike formalism. The system is formed by a collection of Heisenberg spins whose spatial distribution corresponds to a soft sphere fluid with its particle positions frozen at a certain quench temperature. The spin orientations are allowed to equilibrate at a given equilibrium temperature. If the quench and equilibrium temperatures are similar the properties of the positionally frozen system are practically indistinguishable from those of the fully equilibrated Heisenberg spin fluid. On the other hand, one observes that as the quenching temperature of the spatial degrees of freedom increases, so does the Curie temperature of the Heisenberg spins. The theory fails to reproduce the location of the ferromagnetic transition, despite its relative accuracy in the determination of the orientational structure in the supercritical region.

PACS. 75.50.Lk Spin glasses and other random magnets – 64.60.Fr Equilibrium properties near critical points

1 Introduction

The effects of quenching the translational degrees of freedom on the ferromagnetic transition in dipolar fluids have been the focus of various works in recent years [1–4]. Both simulation techniques [1,3], mean field theory [2] and quite recently the Replica Ornstein Zernike (ROZ) integral equation theory [4] have been applied to elucidate the changes induced in the orientational order transition in dipolar fluids by the freezing of the particle positions. In a related work, the authors focused on the ferromagnetic transition of a positionally frozen hard sphere Heisenberg spin system [5]. In reference [5] it was found that the critical behavior is hardly affected by the quenching of the particle positions. Moreover, since in this case the spatial distribution is entirely determined by the hard core repulsions, the ferromagnetic transition cannot be correlated with the temperature at which the particle positions are quenched.

In this work we will focus on a soft core Heisenberg system which quite recently [6] has also being the subject of investigation in the fully equilibrated –*i.e.* spin fluid – case. The spin-spin interaction in this model is defined by

$$U(r_{12}, \omega_1, \omega_2) = -J(r_{12})(\mathbf{s}_1 \cdot \mathbf{s}_2) \tag{1}$$

with the spin-spin exchange coupling given by

$$J(r) = \epsilon \frac{\sigma}{r} \exp[(\sigma - r)/\sigma],$$

and being $\mathbf{s}_i$ the unit vector that describes the orientation of the spin i. Here ϵ is always positive, favoring ferromagnetic alignment.

For practical purposes $J(r)$ is truncated and shifted at $R = 2.5\sigma$, so that $J(r) = 0$ for $r \geq R$. The spatial distribution of the spins corresponds to that of a frozen soft sphere fluid interacting *via*

$$\psi_{soft}(r) = 4\epsilon \left[\left(\frac{\sigma}{r}\right)^{12} - \left(\frac{\sigma}{r}\right)^{6} \right] + \epsilon, \text{ if } r < 2^{1/6}\sigma$$

and $\psi_{soft}(r) = 0$ otherwise, being σ and ϵ the range and energy parameters of this potential. Now, in the present instance the spatial distribution of the spins will be defined by quenching the positions of this soft sphere fluid interacting via $\psi_{soft}(r)$ at a quench temperature $T_0^* = k_B T_0/\epsilon$. As a matter of fact, in the case of Heisenberg interactions, the spatial distribution is hardly sensitive to the spin-spin correlations for temperatures as low as the Curie point. One might envisage then the situation depicted here as the effect of quenching the particle positions on the spin fluid itself.

We will investigate here how the quenching temperature affects the ferromagnetic transition resorting to an

[a] e-mail: E.Lomba@iqfr.csic.es

extensive Monte Carlo study, using a combination of cluster and individual particle moves – *i.e.* spin flips – over a significantly large number of spatial configurations [5]. For this purpose we will here consider spatial distributions corresponding to a soft sphere fluid at a reduced density $\rho\sigma^3 = 0.6$ and high ($T_0^* = 100$), and low ($T_0^* = 2.1$) temperatures. This latter temperature lies close to the Curie point of the corresponding fully equilibrated system. A comparison with the spin fluid results recently presented by Mryglod, Omelyan and Folk [6], will also show here that, as in the hard sphere case of reference [5], the effect of freezing the particle positions is practically negligible. This will not be necessarily so in other systems in which the addition of constrains –such as the freezing of the translational degrees of freedom– might even induce a change in the universality class governing the critical behaviour. This and related issues have been discussed in connection with a Heisenberg system by Kyriakidis and Geldart [7] and Mryglod and Folk [8].

In parallel with the computer simulation study we have also solved the ROZ equations in the Hypernetted Chain (HNC) approximation for this system, which are nothing but a particular case of those equations formulated by Klapp and Patey [4] for positionally frozen dipolar systems. We will see that these equations can accurately reproduce the microscopic structure and internal energy of this model for states away from the ferromagnetic transition, but tend to overestimate by far the Curie temperature. This is in marked contrast with the corresponding HNC equation for the spin fluid, which provides reasonably accurate transition temperatures [9].

The rest of the paper is organized as follows. In the next Section we introduce the ROZ equations for the positionally frozen Heisenberg system. Details of the simulations are presented in Section 3. Finally in Section 4 we present our most significant results and conclusions.

2 The replica Ornstein-Zernike formalism

Following Klapp and Patey [4], the application of the replica trick [10] to a system like ours, in which the orientational degrees are allowed to equilibrate and the particle positions are frozen, reduces to considering the $s \longrightarrow 0$ limit of a fully equilibrated system composed of soft spheres with embedded s replicas of the spins, such that its Hamiltonian reads

$$H^{rep} = \frac{\beta_0}{\beta}\sum_{i>j}\psi_{soft}(r_{ij}) + \sum_{\alpha=1}^{s}\sum_{i>j} J(r_{ij})(\mathbf{s}_i^\alpha \cdot \mathbf{s}_j^\alpha), \quad (2)$$

where $\beta = 1/k_B T$ and $\beta_0 = 1/k_B T_0$, being T_0 and T the temperature at which the particle positions have been frozen, and the equilibrium temperature of the spins, respectively. Note that according to equation (2) only replicas of the same family, α, interact.

The Ornstein-Zernike equation in Fourier space for this replicated system reads

$$\tilde{h}^{rep}(12) = \tilde{c}^{rep}(12) + \rho\int \tilde{c}^{rep}(13)\tilde{h}^{rep}(32)d\{\omega_\mathbf{3}\} \quad (3)$$

where $d\{\omega_3\} = d\omega_3^1 \dots d\omega_3^s$ denotes the integration over the orientations of the s replicas of the spin in particle 3, ρ is the number density, and $\tilde{h}^{rep}$ and $\tilde{c}^{rep}$ the Fourier transforms of the total and direct correlation functions respectively. Given the symmetry of the interaction (1) the replicated functions can simply be expanded in Legendre polynomials to get

$$f^{rep}(12) = \sum_{\alpha\beta}\sum_{l} f_l^{\alpha\beta}(r)P_l\left(\cos\theta_{12}^{\alpha\beta}\right) \quad (4)$$

where the $f_0^{\alpha\beta}(r) = f_0(r)/s^2$, and in general

$$f_l^{\alpha\beta}(r) = \frac{2l+1}{2}\int d\cos\theta_{12}^{\alpha\beta} f^{rep}(12)P_l\left(\cos\theta_{12}^{\alpha\beta}\right). \quad (5)$$

Now, inserting (4) in equation (3) and taking the limit $s \longrightarrow 0$, the ROZ equations read

$$\tilde{h}_0 = \tilde{c}_0 + \rho\tilde{c}_0\tilde{h}_0 \quad (6)$$

$$\tilde{h}_l^f = \tilde{c}_l^f + \frac{\rho}{2l+1}\left[\tilde{c}_l^f\tilde{h}_l^f - \tilde{c}_l^b\tilde{h}_l^b\right] \quad (7)$$

$$\tilde{h}_l^b = \tilde{c}_l^b + \frac{\rho}{2l+1}\left[\tilde{c}_l^f\tilde{h}_l^b + \tilde{c}_l^b\tilde{h}_l^f - 2\tilde{c}_l^f\tilde{h}_l^f\right] \quad (8)$$

where $l \neq 0$, and

$$f_l^b(r) = \lim_{s\longrightarrow 0} f_l^{\alpha\beta}(r) \ \text{ if } \alpha \neq \beta$$

$$f_l^f(r) = \lim_{s\longrightarrow 0} f_l^{\alpha\alpha}(r).$$

As usual, we can define the connected functions by $f^c = f^f - f^b$, by which the last two equations for $l \neq 0$ can be rewritten as

$$\tilde{h}_l^f = \tilde{c}_l^f + \frac{\rho}{2l+1}[\tilde{c}_l^c\tilde{h}_l^f + \tilde{c}_l^b\tilde{h}_l^c] \quad (9)$$

$$\tilde{h}_l^c = \tilde{c}_c^c + \frac{\rho}{2l+1}\tilde{c}_l^c\tilde{h}_c^c. \quad (10)$$

These equations are just a particular case of those derived by Klapp and Patey [4], as can easily be seen from equation (21) of reference [4] if one recalls that for the symmetry of the Heisenberg interaction the rotational invariant coefficients and the Legendre expansion coefficients are simply related by $f^{ll0} = f_l$. Note also that here we have neglected the local order parameters since this type of separable interactions are not likely to produce freezing of the spin axes.

As to the closure relation, here we will focus on the HNC approximation, which reads

$$c^{rep}(12) = h^{rep}(12) - \log[h^{rep}(12) + 1] - \beta u^{rep}(12) \quad (11)$$

where according to (2)

$$\beta u^{rep}(12) = \beta_0\psi_{soft}(r_{12}) + \beta\sum_{\alpha} J(r_{12})(\mathbf{s}_1^\alpha \cdot \mathbf{s}_2^\alpha). \quad (12)$$

The $s \longrightarrow 0$ limit of (11) can be obtained if one uses the following form of the HNC closure [11], expanded in

Legendre's polynomials

$$c_l^{\alpha\beta}(r) = -\beta u_l^{\alpha\beta}(r) - \int_r^\infty dr' \int d\{\frac{\omega_1}{4\pi}\}d\{\frac{\omega_2}{4\pi}\}h^{rep} \times \frac{\partial X^{rep}(12)}{\partial r'} P_l(\cos\theta_{12}^{\alpha\beta}) \quad (13)$$

where $X^{rep}(12) = h^{rep}(12) - c^{rep}(12) - \beta u^{rep}(12)$. This expression, after the replica limit is taken reads

$$c_0(r) = -\beta_0 u_0(r) - \int_r^\infty dr' h_0(r')\frac{\partial X_0(r')}{\partial r'} \quad (14)$$

$$c_l^f(r) = -\beta u_l(r) - (2l+1)\sum_{\lambda\lambda'} \begin{pmatrix} \lambda & \lambda' & l \\ 0 & 0 & 0 \end{pmatrix}^2 \times \int_r^\infty dr' h_\lambda^f(r') \frac{\partial X_{\lambda'}^b(r')}{\partial r'} \quad (15)$$

$$c_l^b(r) = -(2l+1)\sum_{\lambda\lambda'} \begin{pmatrix} \lambda & \lambda' & l \\ 0 & 0 & 0 \end{pmatrix}^2 \times \int_r^\infty dr' h_\lambda^b(r') \frac{\partial X_{\lambda'}^b(r')}{\partial r'} \quad (16)$$

where the quantities in brackets are the $3-j$ Wigner symbols, $u_0(r) = \psi_{soft}(r)$ and $u_1(r) = J(r)$ (with $u_l = 0$ for $l > 1$.) From equations (16) and (6–8) it turns out that $h_l^b = c_l^b = 0$ when $l \neq 0$ (and $h_0^f = h_0^b = h_0$ by definition). With this, the equations can be recast in a form more suitable for our purposes

$$h_0(r) = \exp[-\beta_0 u_0(r) + s_0(r)] - 1 \quad (17)$$

$$h_l^f(r) = \frac{2l+1}{2}\int d\cos\theta P_l(\cos\theta)(h_0(r)+1) \times \exp\left[\sum_{l'=1}(-\beta u_{l'}(r) + s_{l'}^f(r))P_{l'}(\cos\theta)\right] \quad (18)$$

where, as usual, $s = h - c$, and equation (18) holds for $l > 0$. Equation (6) can be solved coupled with (17) and this gives the spatial distribution of the soft sphere fluid at the quenching inverse temperature β_0. Equations (7) and (18) will describe the orientational structure of the spins at the equilibrium inverse temperature β.

3 Simulation details

We have performed simulations using a combination of a local update algorithm with a cluster algorithm as performed in reference [5]. The local update algorithm is tailored so as to directly generate configurations (*i.e.* spin orientations) within the canonical ensemble. As to the cluster algorithm, it is essentially based on the method of Swendsen and Wang [12].

In our particular case, we have to generate a given spatial distribution of the spins, using a canonical simulation of a system interacting *via* $\psi_{soft}(r)$ at a reduced quench temperature $T_0^* = kT_0/\epsilon$ and perform a given number of local updates and cluster moves. After the thermal average one has to average over topological disorder and the accuracy of the results depends on both factors. For a reduced quench temperature $T_0^* = 2.1$ we performed calculations using 55 independent spatial configuration, with thermal averages carried out along 10^5 moves, after 5×10^4 equilibration orientational moves. Each orientational move implies N local spin updates (where N is the number of particles) and a cluster move. The results obtained were compared with those of a simulation in which disorder averages were performed over 200 configurations and thermal averages over 10^3 orientational moves preceded by 10^3 equilibration moves. We found out that the results were indistinguishable within the error bars. Actually, another simulation run using only one tenth of these orientational moves produced results that deviate a mere 0.2% in the critical temperature. Consequently, all results presented in what follows correspond to the simulation that uses 200 configurations and 2×10^3 orientational moves of which the first half correspond to the equilibration period.

From the simulation results it is possible to perform a finite size scaling (FSS) analysis, for which it is necessary to evaluate Binder's cumulant [13]

$$U_4 = 1 - \frac{\langle m^4\rangle}{3\langle m^2\rangle^2}, \quad (19)$$

where the magnetization per particle is defined by

$$m = \frac{1}{N}\left|\sum_j^N \mathbf{s}_i\right|.$$

Binder's parameter must be calculated for various sample sizes in order to perform the FSS analysis. Here we have considered samples of 256, 500, 864, 1372 and 4000 particles. Plotting U_4 *vs.* the equilibrium $T^* = k_BT/\epsilon$ for various sample sizes, the crossing of the U_4 curves determines the location of the critical temperature, T_c^*. Since simulations were run only for a reduced number of temperatures around T_c^*, we applied the histogram reweighting technique to interpolate between the simulated temperatures [14].

As in reference [5], the FSS analysis can also be applied to a quantity like the percolation fraction, ϕ, defined as the fraction of configurations in which there is at least one Swendsen-Wang cluster that percolates through the periodic system. Note however, that since the cluster definition depends on the temperature, one cannot make use of the histogram reweighting technique in this case. Therefore, here we have resorted to a simple mathematical interpolation procedure. Since polynomial fittings introduced undesired features on the interpolated results, we used a function of the type

$$\phi = a_0(1 - \tanh[a_1(T^* - a_2)]) + a_3,$$

where the four a_i's were determined to fit the values of ϕ for the various temperatures around T_c^* at which the simulations were run.

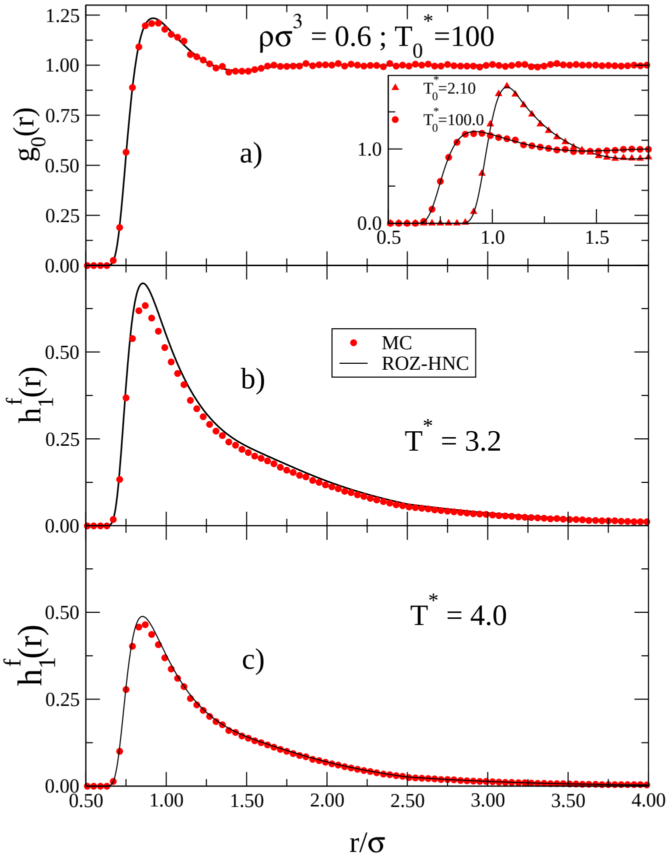

Fig. 1. Leading coefficients of the pair distribution function of the positionally frozen Heisenberg spin system at two temperatures. a) Radial distribution function, $g_0(r) = h_0(r) + 1$, corresponding to a soft sphere fluid quenched at $T_0^* = 100$ b) $h_1^f(r)$ coefficient of the spin-spin pair distribution function at $T^* = 3.2$ c) same as b) at $T^* = 4.0$. The inset in Figure a) illustrates the two radial distribution functions of the soft sphere fluid quenched at high and low temperatures.

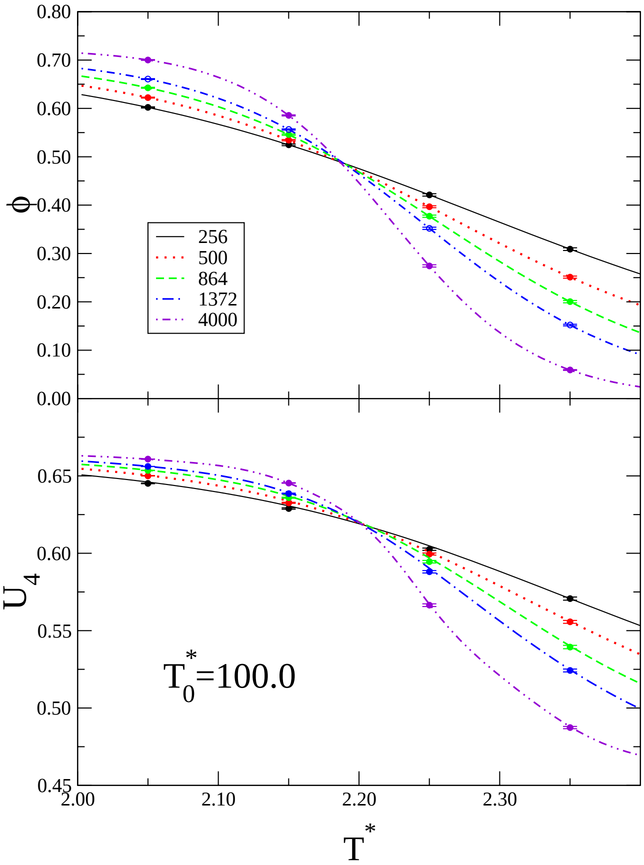

Fig. 2. Evolution of Binder's cumulant, U_4, and percolation fraction,ϕ, with temperature and system size for a positionally frozen Heisenberg system with the spatial distribution of a soft sphere fluid quenched at $T_0^* = 100.0$.

4 Results

As a preliminary study, we have reproduced one of the spin fluid calculations carried out in reference [6], namely the state at density $\rho\sigma^3 = 0.6$, for which Mryglod and coworkers obtained a critical temperature $T_c^* = 2.054 \pm 0.001$ with a critical $U_u = 0.619 \pm 0.002$. Our calculations using only 1372 and 2048 particle samples, yield an estimate of $T_c^* = 2.059$ with $U_4 = 0.615$ using Binder's cumulant analysis and $T_c^* = 2.054$ from the analysis of the percolation fraction. The agreement is sufficiently satisfactory to conclude that the simulation procedure is reliable. For this ferromagnetic transition, the HNC approximation predicts a critical temperature $T_c^* = 2.187$, which overestimates the simulation results by a 6%.

Figure 1 illustrates the ability of the ROZ-HNC approximation to capture the orientational structure of the positionally frozen spin system. The spatial distribution of the spins corresponds to quenched configurations of a soft sphere fluid at $T_0^* = 100$ and $\rho\sigma^3 = 0.6$. It is easily appreciated that the structure is rather well reproduced at high temperatures. As the temperature is lowered the ROZ angular correlation becomes somewhat more long ranged. Now, if the temperature is further lowered the integral equation breaks down and predicts a ferromagnetic transition at $T_{ns}^* = 2.826$ well above the Curie temperature of the spin fluid at the same density. This can be understood if one realizes that particles can be much closer (and consequently angular correlations much stronger) when the spatial distribution corresponds to a high temperature system–compare the high and low temperature distribution functions in the inset of Figure 1a. When one uses a $g_0(r)$ obtained by quenching the soft sphere fluid at $T_0^* = 2.1$, the ROZ-HNC equation breaks down at $T_{ns}^* = 2.42$, which is well above the Curie temperature of the fluid but below the non-solution temperature for the high temperature quench. In any case, we will see that the ROZ overestimates the Curie temperature for both positionally frozen systems and this is in clear contrast with the reasonable estimates obtained for the spin fluid in the HNC approximation. In fact, already at $T^* = 3.2$ the ROZ $h_1^f(r)$ can be seen to decay more slowly than its simulated counterpart and it is then not surprising that this enhanced long ranged angular correlations induce a transition in the theoretical results in conditions where the simulation still yields a fully isotropic system.

Table 1. Critical parameters of positionally frozen Heisenberg systems corresponding to spatial distributions from a soft sphere fluid quenched at high and low temperature. The various critical temperature estimates are obtained from different sources as indicated in the text and in the table with the symbols in parenthesis. The spin fluid FSS results are from reference [6] and the corresponding non-solution T^*_{ns} is obtained in the HNC approximation.

T^*_0	$T^*_c(U_4)$	$T^*_c(\phi)$	$T^*_c(m_c)$	U_4	$\gamma/\nu(\chi)$	$\gamma/\nu(\beta/\nu)$	β/ν	T^*_{ns}
100.0	2.196(3)	2.189(2)	2.193(2)	0.618(2)	1.93(2)	1.98(8)	0.51(4)	2.826
2.1	2.050(6)	2.042(4)	2.050(3)	0.617(2)	1.92(2)	1.96(8)	0.52(4)	2.420
spin fluid	2.054(2)	–	2.057	0.619(2)	1.90(3)	1.92(4)	0.54(2)	2.187

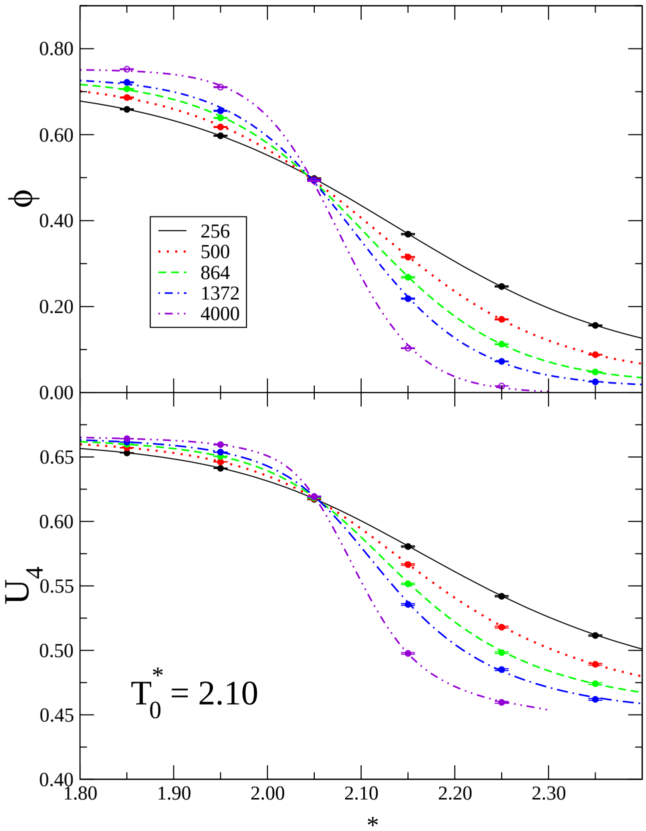

Fig. 3. Evolution of Binder's cumulant, U_4, and percolation fraction,ϕ, with temperature and system size for a positionally frozen Heisenberg system with the spatial distribution of a soft sphere fluid quenched at $T^*_0 = 2.1$.

As to the internal energy, for $T^* = 4.0$ the integral equation predicts a value $U/Nk_BT = -0.075$ in good agreement with the MC value -0.073. Larger discrepancies are found as the temperature is lowered, and thus for $T^* = 3.2$ the ROZ result is $U/Nk_BT = -0.142$ in contrast with the MC value -0.131.

Let us now focus on the analysis of the simulation results for the two quenched systems under consideration. In Figure 2 we present the evolution of Binder's cumulant, U_4, and the percolation fraction, ϕ, for various system sizes when the spatial distribution of the spins corresponds to the high temperature quench, $T^*_0 = 100$. Following reference [15] we fit the temperatures at the intersection of the 256 and 512 curves with the remaining curves to $T_i(b) = T^*_c + c/\log b$ where $b = (N/256)^{1/3}$ for the 256 curve intersections and $b = (N/512)^{1/3}$ for the 512 case. The T^*_c values resulting from both fits agree within statistical accuracy. This comes to suggest that the linear fit is adequate, despite the fact that non-linear corrections should be added when $b-1$ is not small [13], which is the case here for some sample sizes. The use of the linear fit in similar situations is common practice in the literature [15–17].

The results obtained from U_4 and ϕ are collected in Table 1, and tell us that the critical temperature of this frozen system is somewhat above that of the spin fluid system (2.059), but well below the ROZ predictions. Additionally, one can also obtain an estimate of the critical temperature from the system size dependence of the critical magnetization m_c, which is know to scale as $m_c \propto L^{-\beta/\nu}$, with β and ν the magnetization and correlation length exponents respectively [13]. Again in Table 1 we find the results from this analysis to be in good agreement with the U_4 and ϕ estimates of T^*_c. The critical exponent γ/ν is determined from a fit of the magnetic susceptibility $\chi = L^3(\langle m^2\rangle - \langle m\rangle^2))/k_BT$, since its maxima scale with sample since as $\chi_m \propto L^{\gamma/\nu}$. The result of the fit is denoted in Table 1 by $\gamma/\nu(\chi)$. If one calculates $\gamma/\nu = 3 - 2(\beta/\nu)$ one obtains the value shown in Table 1 under $\gamma/\nu(\beta/\nu)$, which agrees with the result of the fit within the error bars.

A similar analysis carried out for the low temperature quench, $T^*_0 = 2.1$ leads to the results of the second row of Table 1. Now one sees that the critical temperature is somewhat lower and other critical parameters are independent of the quenching temperature. The critical temperature is in fact nearly identical to that of the spin fluid, which is an indication that the quenching of particle positions in this case of separable angular interactions does not affect the critical behavior, as was also found for the hard sphere Heisenberg system in reference [5]. Aside from T^*_c, the critical parameters for both spatial distributions agree with those reported by Mryglod and coworkers [6] for the spin fluid. As to the ROZ critical temperatures, we may remark one last point. Despite its overestimation of the Curie temperature, the theory reproduces the correct qualitative trend in the dependence of T^*_c with the topology, namely, the high temperature quench has a higher Curie temperature both in the simulation results and in the ROZ calculations.

In summary, we have seen that the ROZ-HNC approximation reproduces with reasonable accuracy the structure of the positionally frozen Heisenberg system at temperatures above the ferromagnetic transition, reproduces qualitatively the increase in the Curie temperature associated with the rise in the quenching temperature, but clearly overestimates the transition temperatures. This overestimation is in part due to what can be considered the main deficiency of the ROZ-HNC approximation in this system: whereas the simulation clearly indicates that freezing the particle positions does not alter the critical temperature, the ROZ results show a substantial increase in T_c^*. As to the simulation results, one can conclude that, aside from the critical temperature, the remaining critical parameters of the positionally frozen Heisenberg system are practically indistinguishable from those obtained for the Heisenberg spin fluid.

The authors acknowledge support from the Dirección General de Investigación Científica y Técnica under grant No. BFM2001-1017-C03-01 (EL and CM), and No. MAT2002-04540-C05-03/05 (NGA).

References

1. G. Ayton, M.J.P. Gringas, G.N. Patey, Phys. Rev. Lett. **75**, 2360 (1995)
2. H. Zhang, M. Widom, Phys. Rev. B **51**, 8951 (1995)
3. G. Ayton, M.J.P. Gringas, G.N. Patey, Phys. Rev. E **56**, 562 (1997)
4. S.H.L. Klapp, G.N. Patey, J. Chem. Phys. **115**, 4718 (2001)
5. E. Lomba, C. Martín, N.G. Almarza, Mol. Phys. **101**, 1667 (2003)
6. I.M. Mryglod, I.P. Omelyan, R. Folk, Phys. Rev. Lett. **86**, 3156 (2001)
7. J. Kyriakidis, D.J.W. Geldart, Phys. Rev. B **53**, 11572 (1998)
8. I.M. Mryglod, R. Folk, Physica A **294**, 351 (2001)
9. E. Lomba, J.J. Weis, N.G. Almarza, F. Bresme, G. Stell, Phys. Rev. E. **49**, 5169 (1994)
10. S.F. Edwards, R.C. Jones, J. Phys. A **9**, 1595 (1976)
11. P.H. Fries, G.N. Patey, J. Chem. Phys. **82**, 429 (1985)
12. R.H. Swendsen, J.S. Wang, Phys. Rev. Lett. **58**, 86 (1987)
13. K. Binder, Z. Phys. B **43**, 119 (1981)
14. A.M. Ferrenberg, R.H. Swendsen, Phys. Rev. Lett. **63**, 1195 (1989), R.H. Swendsen, Physica A **194**, 53 (1993)
15. J.J. Weis, M.J.P. Nijmeijer, Phys. Rev. Lett. **75**, 2887 (1995)
16. P. Peczak, A.M. Ferrenberg, D.P. Landau, Phys. Rev. B **43**, 6087 (1991)
17. C. Holm, W. Janke, Phys. Rev. B **48**, 936 (1993)